

Optimal Feature Point Selection and Automatic Initialization in Active Shape Model Search

Karim Lekadir and Guang-Zhong Yang

Visual Information Processing, Department of Computing
Imperial College London, United Kingdom
{lekadir, gzy}@doc.ic.ac.uk

Abstract. This paper presents a novel approach for robust and fully automatic segmentation with active shape model search. The proposed method incorporates global geometric constraints during feature point search by using inter-landmark conditional probabilities. The A* graph search algorithm is adapted to identify in the image the optimal set of valid feature points. The technique is extended to enable reliable and fast automatic initialization of the ASM search. Validation with 2-D and 3-D MR segmentation of the left ventricular epicardial border demonstrates significant improvement in robustness and overall accuracy, while eliminating the need for manual initialization.

1 Introduction

Active Shape Models (ASM) [1] are well recognized for their ability to capture significant and complex variability within a family of anatomical shapes. They can also act as a deformable template for medical image segmentation, where the search procedure involves in an iterative manner the identification of target feature points followed by the ASM model fitting. The method, however, is also known to have a number of difficulties in practice. First, the ASM search requires a suitable initialization to achieve satisfactory convergence. Generally, this is carried out by subjective manual interaction through which the user places the mean shape close to the anatomical structure under investigation. For shapes with complex geometry or shape variability, this may not be a satisfactory initialization and the search may be trapped in a local minimum. Some global search methods have been investigated for automatic initialization [2,3] but they are time consuming especially in 3-D. Another common problem with the ASM search is the presence of outliers, *i.e.*, when some of the detected feature points lie on incorrect boundary positions, a situation that is inevitable in practice due to confusing or missing image structures. These misplaced points significantly affect the segmentation outcome due to the least squares minimization nature of the subsequent pose and shape parameters estimation. Some robust ASM extensions have been suggested [4,5] but their performance is limited depending on the level of noise, as well as the dimensionality and complexity of the problem. Finally, the feature point detection is traditionally carried out using normal search profiles, which are not guaranteed to cover the features of interest on the boundary, as these types of search regions lack tangential coverage. Consequently, some target

structures may not be reached at any iteration of the search procedure and some additional manual interaction may be necessary to define key landmarks, such as the valve and apex points in long axis left ventricular segmentation.

These three challenges are addressed in this paper within a single framework. The fundamental theoretical basis behind this work is the optimal feature point selection algorithm, based on inter-landmark conditional probabilities and the A* graph search algorithm. Instead of selecting the feature candidates with the best grey-level properties within each search region independently, the proposed algorithm finds in one step the least grey-level cost and geometrically consistent combination of feature candidates from all search regions, ensuring the elimination of erroneous feature points. The optimality of the algorithm enables the use of large search regions instead of the normal search profiles, resulting in extended coverage of the target features and improved adaptation to complex structures. With some modifications, the proposed algorithm allows reliable and fast automatic initialization of the ASM search without user interaction. The validation is carried out on the challenging MR segmentation of the left-ventricular epi-cardial border both in 2-D and 3-D.

2 Methods

2.1 Optimal Feature Point Selection

In ASM search, the feature point selection is achieved by estimating for the candidate points p_{ij} within each search region H_i the degree of match between the underlying grey-level profile and its corresponding model built during the training stage. The grey-level cost function $d_g(p_{ij})$ used for this purpose can be derived for example by calculating the Mahalanobis distance to the mean grey-level profile [6].

In addition to the grey-level based cost function, the proposed framework introduces for optimal feature point selection the notion of inter-landmark conditional probability, which describes the statistical distribution of a landmark point p_i given the known positions of a set of m points (out of n landmark points in the shape), *i.e.*,

$$P(p_i | p_{s(1)}, \dots, p_{s(m)}) = P(\mathbf{x}_i | \mathbf{x}_{s(1)}, \dots, \mathbf{x}_{s(m)}) \quad (1)$$

where s is an indexing function and \mathbf{x}_i denotes the coordinates of the point p_i . The estimation of the conditional p.d.f. requires a suitable regression model that relates the points p_i and $p_{s(1)}, \dots, p_{s(m)}$. Based on a generalization of the barycentric coordinates [7], the introduced formulation describes \mathbf{x}_i as an affine combination of $\mathbf{x}_{s(1)}, \dots, \mathbf{x}_{s(m)}$ which is invariant to the position of the points, as follows:

$$\mathbf{x}_i = \sum_{k=1}^m c_k \mathbf{x}_{s(k)} + \mathbf{t} + \mathbf{e} \quad \text{with} \quad \sum_{k=1}^m c_k = 1 \quad (2)$$

The weights c_k and translation vector \mathbf{t} are calculated at the training stage by differentiation such that the model residuals \mathbf{e} are minimized. With the proposed

landmark-based regression model, the probability density function of \mathbf{x}_i conditioned on the known values of $\mathbf{x}_{s(1)}, \dots, \mathbf{x}_{s(m)}$ can be described using a multivariate Gaussian distribution with mean \mathbf{x}_i^* and covariance \mathbf{S}_i^* :

$$\mathbf{x}_i^* = \sum_{k=1}^m c_k \mathbf{x}_{s(k)} + \mathbf{t} \quad \mathbf{S}_i^* = \text{Cov}(\mathbf{e}_i) \tag{3}$$

The inter-landmark conditional probabilities incorporate geometric constraints to the feature point selection in order to ensure that erroneous feature points are not considered during the procedure. A domain $A(p_i | p_{s(1)}, \dots, p_{s(m)})$ of geometrically allowable candidates for the point p_i can be derived at each stage of the algorithm given the points $p_{s(1)}, \dots, p_{s(m)}$:

$$A(p_i | p_{s(1)}, \dots, p_{s(m)}) = \left\{ \mathbf{x}_{ij} \mid (\mathbf{x}_{ij} - \mathbf{x}_i^*)^T \mathbf{S}_i^{*^{-1}} (\mathbf{x}_{ij} - \mathbf{x}_i^*) < U \right\} \tag{4}$$

where U is a threshold that controls the size of the landmark allowable domain and which can be calculated from the chi-squared distribution [8].

The aim of the proposed algorithm is to select the least grey-level cost set of candidate points amongst all geometrically consistent combinations. For this purpose, a tree search algorithm based on the A^* algorithm [9] is introduced for optimal feature point selection. Let s be the sequence function describing the order in which search regions are explored and starting from the initial region $H_{s(1)}$, a number of paths can be explored. All the paths are stored in a priority queue Q and at each stage of the algorithm, the choice of the path to be further expanded is based on the calculation of a cost function of the actual path g and a heuristic estimation h of the remaining cost to reach the final landmark point. The cost function is calculated by summing all individual grey-level costs in the actual path:

$$g(L_k) = \sum_{i=1}^{|L_k|} d_g(p_{s(i)L_k(i)}) \tag{5}$$

where $|L_k|$ denotes the size of the path L_k and $L_k(i)$ the index of the feature candidate selected within the corresponding search region.

The heuristic function estimates the most optimistic remaining cost to reach the final landmark point, by summing the minimum grey-level cost amongst the geometrically consistent candidates within each remaining search region, *i.e.*,

$$h(L_k) = \sum_{i=|L_k|+1}^n \min_j \left[d_g(p_{s(i)j}) \right] \tag{6}$$

with $p_{s(i)j} \in A(p_{s(i)} | p_{s(1)}, \dots, p_{s(i-1)}) \cap H_{s(i)}$

The cost function g favors paths with the best grey-level characteristics, whilst the heuristic function h is used to penalize paths that lead to poor intensity characteristics within the remaining landmark allowable domains. At each stage of the algorithm, the path L_k with the minimal sum of the cost and heuristic functions is selected from the priority queue, *i.e.*,

$$L_k = \arg \min_{L_k \in Q} [g(L_k) + h(L_k)] \quad (7)$$

The expansion of each path is only allowed using feature candidates that are geometrically consistent with the points in the current path based on the allowable conditional domain in Eq. (4). The tree search is carried out until a path reaches one of the candidates of the last search region $H_{s(n)}$. Because the heuristic in Eq. (6) is admissible, *i.e.*, it never overestimates the remaining cost to the final feature point, it can be shown [9] that the selection achieved using the A* algorithm is optimal and therefore is guaranteed to be the best valid set of feature points within the search regions.

The order in which the search regions are visited in the tree can be defined at the training stage as follows. The first point $p_{s(1)}$ is preferably chosen as a key landmark (corner or high curvature point). Then the i^{th} index in the sequence s corresponds to the point that correlates most with the points already in the sequence, *i.e.*, the point with the smallest allowable domain calculated from the inter-landmark conditional probability $P(\mathbf{x}_{s(i)} | \mathbf{x}_{s(1)}, \dots, \mathbf{x}_{s(i-1)})$. This is equivalent to choosing the point with the minimal determinant of the covariance matrix calculated from Eq. (3). The procedure continues until all n landmark points indices are within the sequence.

It is worth noting that the conditional probability $P(\mathbf{x}_{s(i)} | \mathbf{x}_{s(1)}, \dots, \mathbf{x}_{s(i-1)})$ can be approximated by using only a subset of the points $p_{s(1)}, \dots, p_{s(i-1)}$ that most correlates with the point $p_{s(i)}$. Furthermore, the effect of rotation and scaling is eliminated by using the values from the initialization.

2.2 Automatic Initialization

As a result of the optimality of the introduced algorithm, the method is guaranteed to output the geometrically valid set of feature points with the best intensity profiles independently of the size of the input search regions. This enables the use of considerably large search regions instead of the traditional normal search profiles. By using the entire image for each feature search region, it is evident that the ASM initialization becomes unnecessary. Such a method, however, would require a lot of computations to reach the final solution and is therefore not desirable. The automatic initialization can be significantly speeded up by finding one or a few potential candidates for the initial points $p_{s(1)}$ and then deriving search regions for all other landmark points by estimating the inter-landmark conditional probabilities $P(p_{s(i)} | p_{s(1)})$ and the corresponding allowable domains. To this end, the entire image or a region of interest is scanned and the positions with high heuristic values as calculated from Eq. (7) are eliminated, as

this indicates that the induced landmark allowable domains are unlikely to intersect with the target features. The remaining candidates in the image with low heuristic values, on the other hand, are very likely to lie close to the true position of $p_{s(1)}$. To achieve faster elimination of incorrect initial points, the heuristic is replaced by an average minimal grey-level cost calculated over the m_k first search regions:

$$h_0(p_{s(1)k}) = \frac{1}{m_k} \left[d_g(p_{s(1)k}) + \sum_{i=2}^{m_k} \min_j \left[d_g(p_{s(m_k)j}) \right] \right] \quad (8)$$

with $p_{s(m_k)j} \in A(p_{s(m_k)} \mid p_{s(1)k})$

At the start of automatic initialization, all candidates for the initial point are stored in a priority queue with m_k set to 1. At each subsequent iteration, the candidate with the lowest heuristic value calculated from Eq. (8) is further considered by incriminating its m_k and updating the heuristic accordingly. With this method, candidates inducing landmark allowable domains that intersect the target boundary are brought forward in the priority queue and the algorithm stops when the first few candidates in the priority queue reaches a value of m_k equal to n . The optimal feature point selection algorithm from previous section is then applied to the identified initial points and to the corresponding landmark allowable domains and the result followed by model fitting is used as the ASM initialization.

It must be noted that if the initial orientation and scaling are not known, these can be also efficiently estimated by using the exact same approach presented in this section, by copying the candidate points for different rotations and scale factors and calculating the inter-landmark allowable domains and the heuristic in Eq. (8) accordingly. In left ventricular segmentation with MR, the intersection between the horizontal and vertical long axis views provides initial estimates of these parameters and allows the definition of a region of interest. Typically, the automatic initialization procedure and one iteration of the proposed ASM technique are sufficient to obtain satisfactory convergence. The automatic initialization step is carried out within a few seconds in both 2-D and 3-D.

2.3 Validation

The proposed fully automatic ASM framework is validated with 2-D and 3-D segmentation of the epi-cardial border of the left ventricle from long and short axis MR images. In cardiac MR, reliable segmentation of the epi-cardial boundary without user interaction is challenging because of its intensity appearance that displays faint/weak edges often surrounded by fat and confusing structures. Additionally, the automatic definition of the valve and apex points is difficult.

The LV datasets were collected by scanning 20 subject (13 normal, 5 locally abnormal, 2 severely abnormal) using a 1.5T MR scanner (Sonata, Siemens, Erlangen Germany) and a TrueFISP sequence (TE = 1.5 ms, TR = 3 ms, slice thickness = 10 mm, pixel size of 1.5 to 2 mm) within a single breath-hold. The long and short axis images were annotated by an expert clinician using a manual contouring tool. The estimation of the inter-landmark conditional probabilities and their evaluation using

the proposed ASM framework were carried out on a leave-one-out basis. For automatic initialization, the initial point $P_{s(1)}$ was chosen as the apex for the 2-D segmentation and as the lower RV/LV junction point of the mid-ventricular slice for the 3-D case. For comparison, the datasets were also segmented using the original ASM [1] and a robust ASM extension [4] based on robust estimators. These methods were initialized by placing the mean shapes for each long and short axis image at the centre of the corresponding manual segmentations. The same local intensity models and grey-level cost function was used for all methods, based on the standard ASM search formulation [6].

3 Results

Table 1 summarizes the segmentation error statistics (mean, standard deviation, min and max) for both the 2-D and 3-D epi-cardial datasets, as obtained using the existing ASM methods, the automatic initialization alone and the entire proposed ASM framework. To aid visualization, the segmentation errors for the 20 datasets are also displayed for the 3-D case in Fig. 1. It can be seen from the results that the original ASM lacks robustness for epi-cardial segmentation, as the target structures, unlike the endo-cardial borders, are often poorly defined and coupled with considerable artifacts. The robust ASM improves upon the original ASM results (14 % average improvement in 2-D and 22 % in 3-D), but its performance is not consistent for all datasets. It is evident from the obtained results that the proposed fully automatic framework outperforms the existing techniques used for comparison. In particular, it can be seen that on average the automatic initialization alone performs better in shape localization, which demonstrates its robustness. The entire framework using automatic initialization and the optimal feature selection performs well for all datasets, with a maximal segmentation error less than 2 mm and an average improvement with respect to ASM of 46 % and with respect the robust ASM of 33 %. This performance can be explained by the nature of the proposed method, which ensures outlier-free image search due to the geometrically constrained selection of feature points, while existing ASM methods become more instable as the imaging conditions or the boundary appearance characteristics deteriorate.

Fig. 2 shows 2-D/3-D illustrations of the strength of the proposed algorithm when applied to challenging segmentation tasks. The 2-D long axis view displays a dilated left ventricle with poor signal definition of the boundaries, especially at the apex and lateral apical regions. As a result, the original ASM fails to recover the boundary of

Table 1. Detailed error analysis of the ASM methods (in *mm*)

	2-D				3-D			
	Mean error	Std.	Min error	Max error	Mean error	Std.	Min error	Max error
Original ASM [1]	2.01	1.12	0.87	4.98	2.13	1.01	0.98	4.94
Robust ASM [4]	1.71	0.92	0.86	4.38	1.65	1.00	0.92	4.66
Auto. initialization	1.23	0.32	0.82	1.88	1.60	0.41	0.96	2.67
Proposed method	1.13	0.32	0.64	1.82	1.11	0.25	0.79	1.84

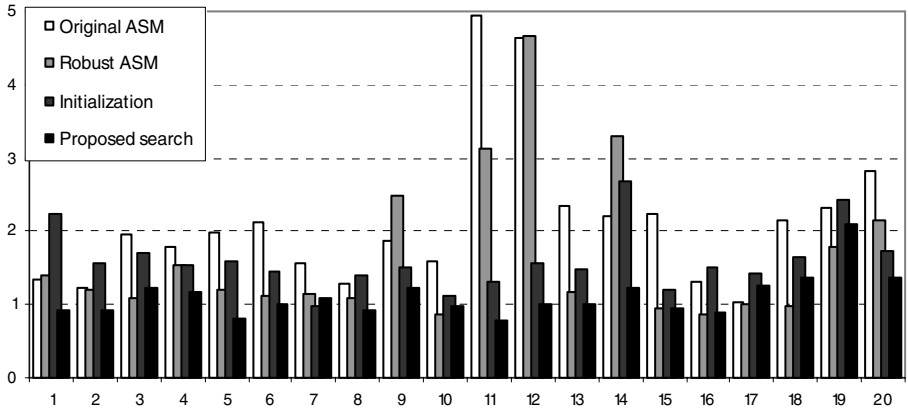


Fig. 1. 3-D segmentation errors (in mm) as obtained with the proposed technique and initialization, with comparison to the existing ASM methods

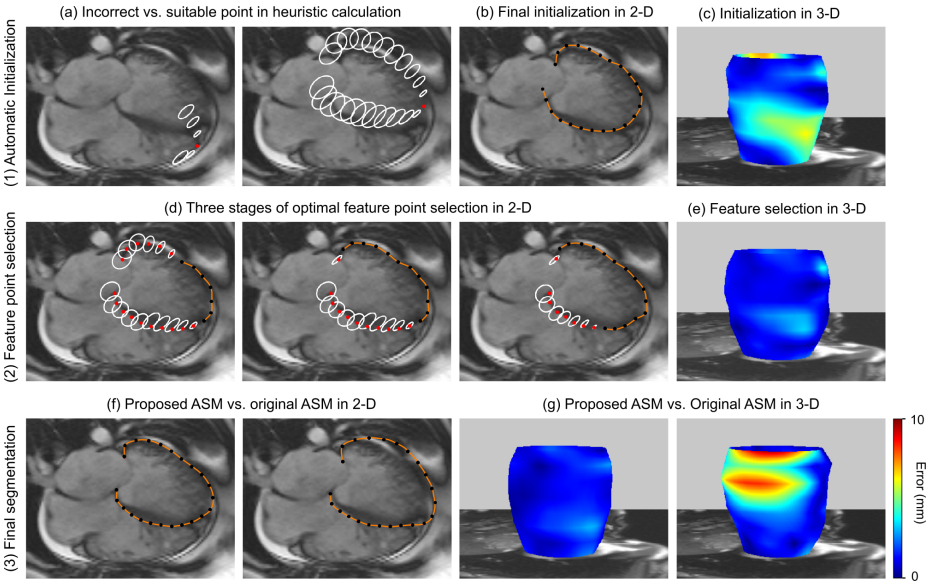


Fig. 2. Illustration of each stage of the proposed technique in 2-D and 3-D

interest (see (f), average segmentation error equal to 4.58 mm). The automatic initialization is illustrated in (a)-(b). The apex of the right ventricle is investigated as a possible initial point due to resemblance with the left ventricular apex. This point is, however, rejected after only a few conditional search regions considered in the heuristic calculation (Eq. (8)), as these landmark allowable domains do not intersect with the target image features, and therefore return high minimal grey-level cost values. In contrast, although the left ventricular apex is poorly displayed in the image, the corresponding allowable domains are located on the boundary of interest and the

candidate point under investigation is therefore successfully selected as an initial point (a). The subsequent final 2-D initialization is shown in (b) after feature point selection. The automatic initialization achieves a reasonably good localization of the boundary, with only minor errors at the apex and valve points. The optimal feature point selection algorithm in subsequent iterations is illustrated in (d), where three intermediate stages of the procedure are shown. It can be noticed that the landmark allowable domains, calculated using the inter-landmark conditional probabilities, become smaller as the path approaches the corresponding landmark points, therefore restricting the selection algorithm to valid candidate positions on the boundary. The final 2-D segmentation is shown in (f), demonstrating high accuracy along the entire boundary, as well as for the key landmark points (valve and apex points). Similarly, the proposed method achieves significant improvement in 3-D (see (g)), due to more suitable initialization (c) and robust identification of the feature points (e).

4 Conclusion

This paper presents a novel technique for robust feature point detection and automatic initialization in ASM-based segmentation. Due to the use of the A* algorithm and inter-landmark conditional probabilities, the introduced method ensures optimal selection of the feature points according to both geometric and appearance criteria. With some modifications in the heuristic calculation, the algorithm enables fast and reliable automatic initialization of the ASM search. The validation on 2-D and 3-D MR segmentation of the left-ventricular epi-cardial border shows significant increase in overall accuracy and robustness, while eliminating the need for manual initialization.

References

1. Cootes, T.F., Cooper, D., Taylor, C.J., Graham, J.: Active shape models - Their training and application. *Computer Vision and Image Understanding (CVIU)* 61, 38–59 (1995)
2. Brejl, M., Sonka, M.: Object localization and border detection criteria design in edge-based image segmentation: automated learning from examples. *IEEE Transactions on Medical Imaging* 19, 973–985 (2000)
3. de Bruijne, M., Nielsen, M.: Shape particle filtering for image segmentation. In: Barillot, C., Haynor, D.R., Hellier, P. (eds.) *MICCAI 2004*. LNCS, vol. 3216, pp. 168–175. Springer, Heidelberg (2004)
4. Rogers, M., Graham, J.: Robust active shape model search. In: Heyden, A., Sparr, G., Nielsen, M., Johansen, P. (eds.) *ECCV 2002*. LNCS, vol. 2353, pp. 517–530. Springer, Heidelberg (2002)
5. Lekadir, K., Merrifield, R., Yang, G.-Z.: Outlier detection and handling for robust 3-D active shape models search. *IEEE Transactions on Medical Imaging* 26, 212–222 (2007)
6. Cootes, T.F., Taylor, C.J.: Active shape model search using local grey-level models: a quantitative evaluation. In: *Proc. British Machine Vision Conf (BMVC)* (1993)
7. Coxeter, H.S.M.: Barycentric coordinates. In: *Introduction to geometry*, 2nd edn., pp. 216–221. Wiley, New York (1969)
8. Becker, C., Gather, U.: The masking breakdown point of multivariate outlier identification rules. *Journal of the American Statistical Association* 94, 947–955 (1999)
9. Russell, S.J., Norvig, P.: *Artificial intelligence: a modern approach*. Prentice-Hall, Englewood Cliffs (2003)